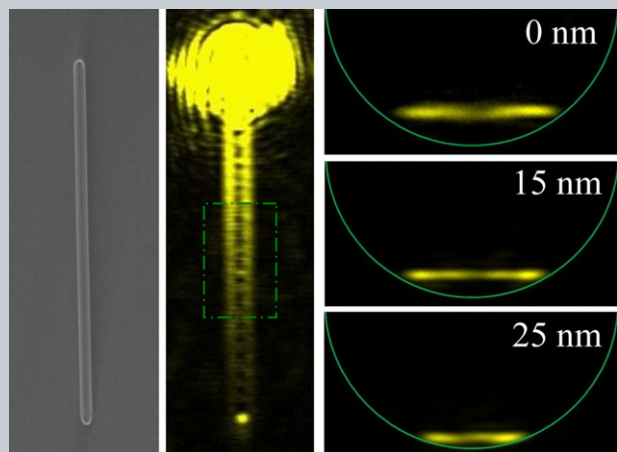


Abstract Metal nanowires supporting propagating surface plasmons (SPs) can be used as nanowaveguides and nanoantennas for light manipulation beyond the diffraction limit. Here the control of the propagation and radiation of SPs on silver nanowires is investigated. By covering an Al_2O_3 layer onto a silver nanowire to change the local dielectric environment, the wave vector of the propagating SPs is increased. Thus, the radiation direction of SPs into the substrate is changed according to the phase matching condition, which is experimentally shown by Fourier imaging method. The radiation angle is sensitively dependent on the Al_2O_3 thickness. By depositing 1 nm Al_2O_3 , the increase of the radiation angle can be close to 1 degree. These results show that dielectric-layer-coating provides a simple and effective method to control the propagation and radiation of SPs, which will be of great importance for designing plasmonic circuits, antennas and sensors based on silver nanowires.



Controlling the radiation direction of propagating surface plasmons on silver nanowires

Zhuoxian Wang¹, Hong Wei^{1,*}, Deng Pan¹, and Hongxing Xu^{1,2}

1. Introduction

Surface plasmons (SPs) are the quanta of collective oscillations of free electrons at metal-dielectric interfaces, which make metal nanostructures show many special optical properties [1, 2]. The excitation of SPs in metal nanostructures can enable the manipulation of light intensity [3–5], polarization [6, 7] and propagation [8, 9] at the nanoscale. Therefore, SPs provide the possibility to miniaturize optical devices to the scale compatible with modern nanoelectronic devices [10] and to build highly integrated nanophotonic circuits [11, 12]. Plasmonic waveguides are the most basic elements for constructing such nanophotonic circuitry. Among the various structures for plasmonic waveguides, chemically synthesized crystalline silver nanowires show low scattering loss for the waveguiding and are widely used in the study of nanowire SP properties [13–21], the interaction between propagating SPs and quantum emitters [22–27], and the coupling between plasmonic and photonic waveguides [28–30]. These wires can support different SP modes with special near-field distributions which have been revealed by fluorescence-based near-field imaging technique [31, 32]. They can be assembled to form branched structures to realize the functions of router and logic gates [32–34].


Putting silver nanowires on a substrate can induce the leakage radiation of SPs to the substrate [35–37]. These substrate-supported Ag nanowires can serve as unidirectional broadband antennas [38]. Precisely controlling the radiation of the nanowire antenna is important for the applications that will benefit from redirecting light toward well-defined directions, such as solar cells and photodetectors [39, 40]. The tunability of the propagating SPs is also crucial for achieving more advanced functions that are essential for on-chip nanophotonic devices. Therefore, developing a simple and reliable method to tune the propagation and radiation of nanowire SPs is of extreme importance. Recently, it is reported that the propagating SPs on silver nanowires are strongly dependent on the surrounding environment, which has been used to tune the near field distribution of SPs for controlling the light routing in nanophotonic circuits [41]. The dependence of SPs on the dielectric environment provides a versatile means to tune the SP propagation and radiation.

In this paper, a simple method is used to modulate the propagation and radiation of SPs on silver nanowires. Using leakage radiation imaging and Fourier imaging methods, we studied the radiation of SPs on silver nanowire into the substrate. The radiation angle is related to the wave vector of the SPs on the nanowire, decided by phase matching

¹ Beijing National Laboratory for Condensed Matter Physics and Institute of Physics, Chinese Academy of Sciences, Beijing 100190, China

² Center for Nanoscience and Nanotechnology, and School of Physics and Technology, Wuhan University, Wuhan 430072, China

*Corresponding author: e-mail: weihong@iphy.ac.cn

 This is an open access article under the terms of the Creative Commons Attribution-NonCommercial-NoDerivs License, which permits use and distribution in any medium, provided the original work is properly cited, the use is non-commercial and no modifications or adaptations are made.

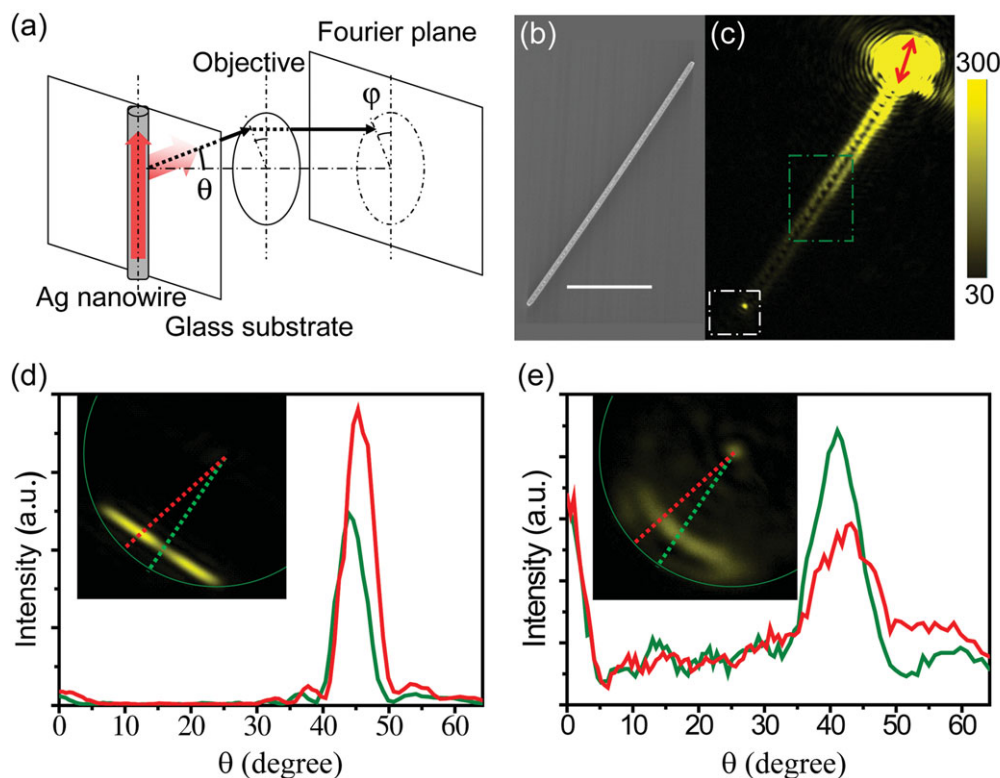


Figure 1 (a) Schematic illustration of the Fourier imaging method. (b) SEM image of a silver nanowire. The scale bar is $5 \mu\text{m}$. (c) Optical propagation image viewed from the glass side. The red arrow shows the polarization of the excitation light of 633 nm wavelength. (d, e) Intensity distribution versus θ along two directions $\varphi = 0$ (green curves) and $\varphi = -15^\circ$ (red curves) on the Fourier images as marked by green and red dashed lines in the insets. The Fourier images are obtained from areas marked by green (d) and white (e) dashed rectangles in (c), corresponding to the radiation from nanowire trunk and terminal, respectively. The green circles on the Fourier images represent the maximum angle θ of radiation that can be collected by the optical system.

condition. By depositing an Al_2O_3 layer to locally change the surrounding environment of the supported silver nanowire, we can tune the wave vector of SPs on the nanowire and the radiation direction. It is found that the radiation angle is sensitively dependent on the thickness of the Al_2O_3 layer. With the increase of Al_2O_3 thickness, the increase of the radiation angle becomes faster. The sensitivity of radiation angle to the Al_2O_3 thickness change is higher for thin nanowires than for thick nanowires, especially when the Al_2O_3 is thick. This dielectric-layer-coating method provides an effective way to control the propagation and radiation of SPs on metal nanowires, which will not only benefit the design of future SP-based devices and circuits, but also provide more possibilities for using plasmonic nanoantennas to redirect light. The highly sensitive response of the radiation angle to the change of the dielectric coating layer can be used for sensing.

2. Leakage radiation from SPs on silver nanowire

The leakage radiation from SPs on silver nanowire is collected and imaged in our experimental setup based on an

upright microscope, as schematically shown in Fig. 1a. The SPs on the glass-supported nanowire can radiate into substrate along with the propagation when the wave vector of the SPs is smaller than the wave vector of light in the substrate. The radiation direction of leakage wave follows the phase matching condition,

$$\text{Re}(k_{\text{sp}/}) = k_{\text{photon}} \cos(\alpha) \quad (1)$$

where $\text{Re}(k_{\text{sp}/})$ is the wave vector of SPs on the nanowire, k_{photon} is the wave vector of photons in the glass substrate, and α is the angle between the leakage radiation direction and the nanowire. The SP radiation into the substrate is collected by an oil immersion objective with a numerical aperture (NA) equals to 1.35. The optical image of the radiation can be directly obtained and the angular intensity distribution $I(\theta, \varphi)$ of the radiation is monitored on the Fourier plane [42], where θ and φ are the angle coordinates denoting the direction of the radiation, as marked in Fig. 1a. The $\varphi = 0$ represents the direction parallel to the measured silver nanowire. The maximum value of θ is restricted by the NA of the objective, i.e. $n_{\text{glass}} \sin(\theta) \leq \text{NA}$. By extracting the radiation angle θ of leakage radiation from the Fourier image, $\text{Re}(k_{\text{sp}/})$ can be obtained from equation (1) since $\alpha = \pi/2 - \theta$ for $\varphi = 0$.

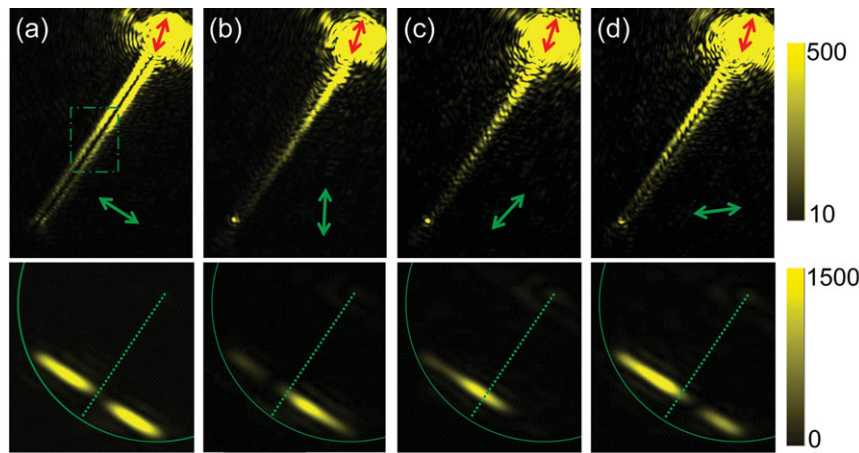


Figure 2 The optical propagation images (top) and corresponding Fourier images (bottom) at certain emission polarizations (green arrows). The signal on the Fourier images comes from the area marked by green rectangle. The red arrows show the polarization of the excitation light. The green circles on the Fourier images represent the maximum angle θ of radiation that can be collected by the system. The green dashed lines are along $\varphi = 0$.

In experiments, the chemically synthesized silver nanowires are deposited on a glass substrate. Laser light of 633 nm wavelength is focused through an oil immersion objective (magnification $100\times$, $NA = 1.35$) onto one end of the nanowire from the glass side to excite the propagating SPs. The signal is collected by the same objective for leakage radiation imaging and Fourier imaging [36]. Figure 1b shows the scanning electron microscopy (SEM) image of a silver nanowire with diameter around 300 nm. Its leakage radiation image in Fig. 1c shows the propagating SPs on the nanowire. The propagating SPs radiate into the substrate, which makes the whole nanowire bright. Certain areas of the silver nanowire are selected by an aperture for Fourier imaging. The obtained Fourier images of the leakage radiation from the propagating SPs on nanowire (green dashed rectangle in Fig. 1c) and of the emitted light from the nanowire terminal (white dashed rectangle in Fig. 1c) are shown in the insets of Fig. 1d and 1e, respectively. The radial intensity distributions along $\varphi = 0$ and $\varphi = -15^\circ$ (green and red dashed lines in Fourier images) are shown in Fig. 1d and 1e. For the radiation from the nanowire trunk, the intensity distribution on Fourier image is in a straight line with a minimum intensity at $\varphi = 0$, which indicates SPs on the nanowire radiate more energy to the two sides. The straight line shape of the Fourier image indicates that the SP wave vector along $\varphi = 0$ direction strictly satisfies the phase matching condition described by equation (1) ($\alpha = \pi/2 - \theta$ for $\varphi = 0$). The radiation angle θ along $\varphi = 0$ is about 44° . For the emission from the nanowire end, the Fourier image is quite different. The intensity distribution is in an arc shape with larger intensity at $\varphi = 0$. The radiation angle θ along $\varphi = 0$ is about 41° . The different emission pattern and angle for the nanowire end may be caused by the SP out-coupling by the scattering at the nanowire end.

The polarization of the leakage radiation on the silver nanowire is further investigated by adding a polarizer into the optical imaging path. For the polarizing axis perpendicular to the silver nanowire, the leakage light is distributed on the two sides of the nanowire (top panel in Fig. 2a). The pattern of the Fourier image (bottom panel in Fig. 2a) splits to two parts with almost no intensity along $\varphi = 0$. This means the radiation along $\varphi = 0$ is polarized parallel

to the silver nanowire. For the polarizing axis parallel to the silver nanowire (Fig. 2c), the intensity mainly concentrates around $\varphi = 0$ with weak intensity observed at the two sides of the nanowire. This means the leakage radiation on the two sides of the nanowire is polarized with large component perpendicular to the silver nanowire. For the polarizing axis along the direction shown by the green arrows in Figs. 2b and 2d, extinction occurs on the left side and right side of the nanowire, respectively. These results indicate that the polarizations of the radiated light from the two sides of the nanowire are almost perpendicular to the directions of green arrows in Figs. 2b and 2d for the left and right side radiation, respectively. The intensity distributions in these four Fourier images clearly show the direction-dependent polarization of the leakage radiation. The radiation to the direction close to $\varphi = 0$ has larger electric field component along $\varphi = 0$ direction.

The direction-dependent polarization of the radiation can be understood by considering the polarization of the SPs on the nanowire. The leaky SP mode on the silver nanowire has both electric field component (E_\perp) perpendicular to the nanowire surface and component (E_\parallel) parallel to the nanowire axis. On the two sides of the nanowire, the perpendicular component E_\perp of SPs is in opposite direction and contributes dominantly to the radiated light. In the direction of $\varphi = 0$, the parallel component E_\parallel of the SPs contributes to the observed radiation.

3. The control of the leakage radiation from supported silver nanowires

According to the phase matching condition between the SPs and photons, the direction of the radiation can be controlled by tuning the wave vector of SPs $\text{Re}(k_{\text{sp}\parallel})$ on the nanowire. In experiments, changing the wave vector of SPs is achieved by coating an Al_2O_3 layer onto the silver nanowire. The Al_2O_3 layer is deposited onto the sample surface using atomic layer deposition (ALD) method so that its thickness can be controlled very precisely. The change of the SP wave vector will result in the change of radiation angle in the Fourier image.

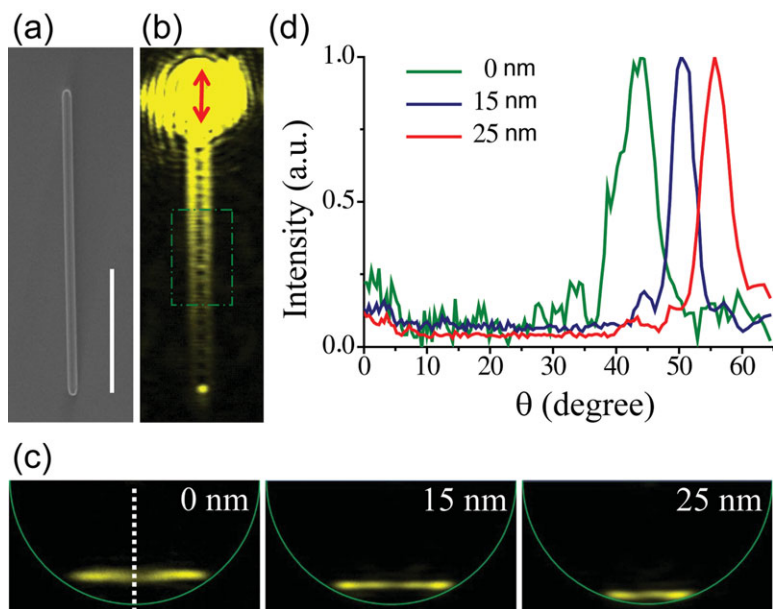


Figure 3 The control of radiation to substrate. (a) SEM image of a silver nanowire. The scale bar is 5 μm. (b) Optical propagation image. (c) Fourier images for different thicknesses of Al₂O₃ layer. (d) Intensity distribution versus θ along $\varphi = 0$ (white dashed line in (c)) corresponding to (c).

Figures 3a and 3b show the SEM image and optical propagation image for a silver nanowire with diameter about 280 nm. The area marked by green dashed rectangle is selected by an aperture for the Fourier images in Fig. 3c with the radial distribution for $\varphi = 0$ shown in Fig. 3d. For the bare nanowire without coating, the radiation angle θ is about 44° at $\varphi = 0$ as shown in Fig. 3c (left panel) and 3d (green curve). By depositing 15 nm thick Al₂O₃ layer, the radiation pattern moves close to the boundary restricted by the objective's NA (green circle in Fig. 3c) and the radiation angle θ at $\varphi = 0$ increases to 50° (middle panel in Fig. 3c and blue curve in Fig. 3d). Then a 10 nm thick Al₂O₃ layer is further deposited on the sample, and the total Al₂O₃ thickness increases to 25 nm. The radiation angle θ at $\varphi = 0$ further increases to 56° (right panel in Fig. 3c and

red curve in Fig. 3d). As can be seen, the SP radiation angle can be largely changed by depositing Al₂O₃ layers onto the nanowire surface.

To provide quantitative description for the dependence of radiation angle on the Al₂O₃ layer thickness, two groups of silver nanowires with diameters in the range of 410–640 nm (thick nanowires) and 200–240 nm (thin nanowires) are further investigated. The leakage radiation angles θ at $\varphi = 0$ versus the thicknesses of Al₂O₃ layer up to 30 nm are plotted in Fig. 4a. Here another objective with NA = 1.40 is used for measuring the samples with 30 nm thick Al₂O₃ layer to better collect the leakage radiation with large angles. In Fig. 4, the green dots are for thin nanowires and the red dots are for thick nanowires. The dots with the same shape and color come from the same nanowire

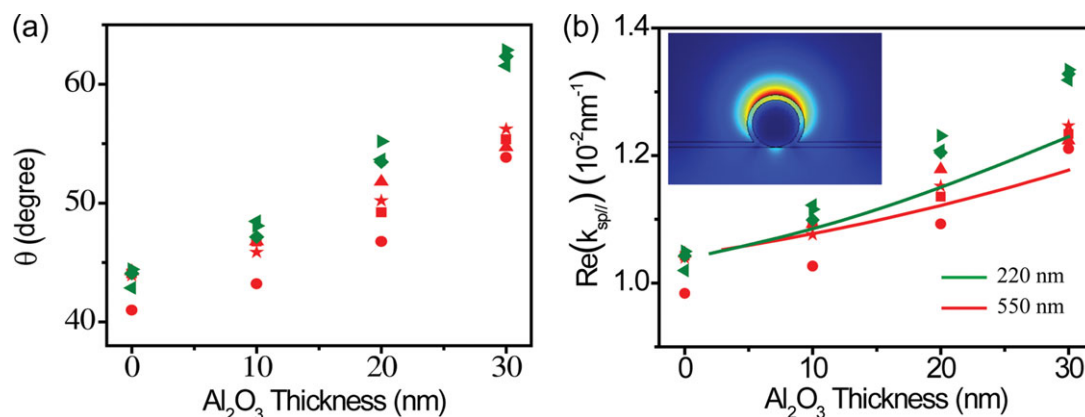


Figure 4 (a) The angles of leakage radiation from supported silver nanowires with different diameters and thicknesses of Al₂O₃ layer. (b) The corresponding $\text{Re}(k_{\text{sp}||})$ of nanowires with different diameters and thicknesses of Al₂O₃ layer. In both (a) and (b), the red dots are measured from thick nanowires with diameters in the range 410–640 nm, while the green dots are from thin nanowires with diameters in the range 200–240 nm. In (b) the green and red curves are the simulation results for nanowires of diameter 220 nm and 550 nm, respectively. The inset shows the electric field intensity distribution of the SP mode leaky to the substrate. The refractive indices used in the simulation are 0.05625+4.276i for Ag, 1.62 for Al₂O₃, and 1.5 for glass substrate.

covered by Al_2O_3 layer of different thicknesses. By increasing the Al_2O_3 thickness from 0 to 30 nm, the leakage radiation angles along $\varphi = 0$ increase gradually for both groups. For thick silver nanowires, the leakage radiation angles are relatively smaller compared to thin nanowires. The dependence of the radiation angle on the Al_2O_3 thickness is quite sensitive. It can be seen from Fig. 4a that the sensitivity is increased with the increase of the Al_2O_3 thickness for the range studied here. By depositing 1 nm thick Al_2O_3 , the radiation angle is averagely increased 0.9° for a nanowire of diameter 220 nm when the Al_2O_3 thickness is changed from 20 nm to 30 nm. The sensitive response of the radiation angle to the local dielectric environment change can be used to design new type on-chip sensors.

The change of leakage radiation angle reflects the alteration of the wave vector of propagating SPs on silver nanowire according to equation (1). The corresponding $\text{Re}(k_{\text{sp}/})$ is calculated and plotted in Fig. 4b. For a single group of silver nanowires (thick or thin), $\text{Re}(k_{\text{sp}/})$ increases with the increase of the thickness of Al_2O_3 layer. This result demonstrates the efficient control of propagating SPs on supported silver nanowire waveguides by slightly changing the dielectric environment. Comparing these two groups of silver nanowires shows that, $\text{Re}(k_{\text{sp}/})$ of thin Ag nanowires is bigger for the same thickness Al_2O_3 layer [41]. By changing the same thickness for the covered Al_2O_3 layer, the change of SP wave vector of thin nanowire is bigger than that of thick nanowire as the electric field is more tightly confined around thin nanowire.

We also calculate the wave vector of the SPs in our structure using finite element method simulation. The electric field distribution of the nanowire SP mode that contributes to the leakage radiation is shown in the inset of Fig. 4b. As can be seen, this mode has a large part of the field distributed on the top of the nanowire and in the air, and it has an effective refractive index lower than the substrate, which means the mode is leaky. The dependence of the wave vector of the mode on the thickness of Al_2O_3 layer is shown by the curves in Fig. 4b, which accords with the experimental result. This also confirms the control of SP propagation and radiation by adding Al_2O_3 layer.

4. Conclusion

In this paper, we demonstrate the precise and efficient control to the radiation direction of propagating SPs on silver nanowire by using Fourier imaging method. This control is achieved by coating silver nanowires with an Al_2O_3 layer deposited by using atomic layer deposition technique. As the dielectric environment of the silver nanowire waveguide is changed by the Al_2O_3 layer, the SP wave vector is changed, which results in the change of angle of radiation to substrate according to the phase matching condition. The radiation angle is found to be sensitively dependent on the thickness of Al_2O_3 layer, which indicates the sensitive dependence of SP wave vector on the Al_2O_3 thickness. Comparing nanowires of different diameters shows that thin nanowires have larger radiation angle and more

sensitive dependence on the Al_2O_3 thickness. As the advanced film deposition techniques can precisely control the thickness of dielectric layers, the layer-coating method reported here provides the reliable and simple control to the propagation and radiation of SPs. This high controllability of propagating SPs on metal waveguides is of great value for the development of plasmonic circuits, and may shed new light on the developments of plasmonic nanoantennas and sensors.

Acknowledgements. We thank Prof. Joachim R. Krenn and Dr. Timur Shegai for the discussions about the Fourier imaging setup. We thank the Laboratory of Microfabrication in Institute of Physics, Chinese Academy of Sciences (CAS) for experimental support. This work was supported by National Natural Science Foundation of China (Grant Nos. 11134013, 11227407, 11004237 and 61210017), The Ministry of Science and Technology of China (Grant No. 2012YQ12006005), Knowledge Innovation Project (Grant No. KJCX2-EW-W04) and Youth Innovation Promotion Association of CAS.

Received: 4 December 2013, **Revised:** 28 January 2014,

Accepted: 14 February 2014

Published online: 12 March 2014

Key words: propagating surface plasmons, silver nanowire, leakage radiation, Fourier imaging.

References

- [1] W. L. Barnes, A. Dereux, and T. W. Ebbesen, *Nature* **424**, 824–830 (2003).
- [2] L. M. Tong, H. Wei, S. P. Zhang, Z. P. Li, and H. X. Xu, *Phys. Chem. Chem. Phys.* **15**, 4100–4109 (2013).
- [3] H. X. Xu, E. J. Bjerneld, M. Kall, and L. Borjesson, *Phys. Rev. Lett.* **83**, 4357–4360 (1999).
- [4] H. X. Xu, J. Aizpurua, M. Kall, and P. Apell, *Phys. Rev. E* **62**, 4318–4324 (2000).
- [5] P. Muhlschlegel, H. J. Eisler, O. J. F. Martin, B. Hecht, and D. W. Pohl, *Science* **308**, 1607–1609 (2005).
- [6] T. Shegai, Z. P. Li, T. Dadosh, Z. Y. Zhang, H. X. Xu, and G. Haran, *Proc. Natl. Acad. Sci. USA* **105**, 16448–16453 (2008).
- [7] Z. P. Li, T. Shegai, G. Haran, and H. X. Xu, *ACS Nano* **3**, 637–642 (2009).
- [8] D. K. Gramotnev and S. I. Bozhevolnyi, *Nat. Photon.* **4**, 83–91 (2010).
- [9] X. Guo, Y. G. Ma, Y. P. Wang, and L. M. Tong, *Laser Photon. Rev.* **7**, 855–881 (2013).
- [10] E. Ozbay, *Science* **311**, 189–193 (2006).
- [11] T. W. Ebbesen, C. Genet, and S. I. Bozhevolnyi, *Physics Today* **61**, 44–50 (2008).
- [12] H. Wei and H. X. Xu, *Nanophoton.* **1**, 155–169 (2012).
- [13] H. Ditlbacher, A. Hohenau, D. Wagner, U. Kreibig, M. Rogers, F. Hofer, F. R. Aussenegg, and J. R. Krenn, *Phys. Rev. Lett.* **95**, 257403 (2005).
- [14] A. W. Sanders, D. A. Routenberg, B. J. Wiley, Y. N. Xia, E. R. Dufresne, and M. A. Reed, *Nano Lett.* **6**, 1822–1826 (2006).

- [15] M. Allione, V. V. Temnov, Y. Fedutik, U. Woggon, and M. V. Artemyev, *Nano Lett.* **8**, 31–35 (2008).
- [16] Z. P. Li, F. Hao, Y. Z. Huang, Y. R. Fang, P. Nordlander, and H. X. Xu, *Nano Lett.* **9**, 4383–4386 (2009).
- [17] Z. P. Li, K. Bao, Y. R. Fang, Y. Z. Huang, P. Nordlander, and H. X. Xu, *Nano Lett.* **10**, 1831–1835 (2010).
- [18] W. H. Wang, Q. Yang, F. R. Fan, H. X. Xu, and Z. L. Wang, *Nano Lett.* **11**, 1603–1608 (2011).
- [19] C. Rewitz, T. Keitzl, P. Tuchscherer, J. Huang, P. Geisler, G. Razinskas, B. Hecht, and T. Brixner, *Nano Lett.* **12**, 45–49 (2012).
- [20] H. Wei and H. X. Xu, *Nanoscale* **4**, 7149–7154 (2012).
- [21] Y. Zhu, H. Wei, P. F. Yang, and H. X. Xu, *Chin. Phys. Lett.* **29**, 077302 (2012).
- [22] Y. Fedutik, V. V. Temnov, O. Schops, U. Woggon, and M. V. Artemyev, *Phys. Rev. Lett.* **99**, 136802 (2007).
- [23] A. V. Akimov, A. Mukherjee, C. L. Yu, D. E. Chang, A. S. Zibrov, P. R. Hemmer, H. Park, and M. D. Lukin, *Nature* **450**, 402–406 (2007).
- [24] Y. R. Fang, H. Wei, F. Hao, P. Nordlander, and H. X. Xu, *Nano Lett.* **9**, 2049–2053 (2009).
- [25] H. Wei, D. Ratchford, X. Q. Li, H. X. Xu, and C. K. Shih, *Nano Lett.* **9**, 4168–4171 (2009).
- [26] R. Kolesov, B. Grotz, G. Balasubramanian, R. J. Stohr, A. A. L. Nicolet, P. R. Hemmer, F. Jelezko, and J. Wrachtrup, *Nat. Phys.* **5**, 470–474 (2009).
- [27] M. Frimmer, Y. T. Chen, and A. F. Koenderink, *Phys. Rev. Lett.* **107**, 123602 (2011).
- [28] X. Guo, M. Qiu, J. M. Bao, B. J. Wiley, Q. Yang, X. N. Zhang, Y. G. Ma, H. K. Yu, and L. M. Tong, *Nano Lett.* **9**, 4515–4519 (2009).
- [29] R. X. Yan, P. Pausauskie, J. X. Huang, and P. D. Yang, *Proc. Natl. Acad. Sci. USA* **106**, 21045–21050 (2009).
- [30] X. Q. Wu, Y. Xiao, C. Meng, X. N. Zhang, S. L. Yu, Y. P. Wang, C. X. Yang, X. Guo, C. Z. Ning, and L. M. Tong, *Nano Lett.* **13**, 5654–5659 (2013).
- [31] S. P. Zhang, H. Wei, K. Bao, U. Hakanson, N. J. Halas, P. Nordlander, and H. X. Xu, *Phys. Rev. Lett.* **107**, 096801 (2011).
- [32] H. Wei, Z. P. Li, X. R. Tian, Z. X. Wang, F. Z. Cong, N. Liu, S. P. Zhang, P. Nordlander, N. J. Halas, and H. X. Xu, *Nano Lett.* **11**, 471–475 (2011).
- [33] Y. R. Fang, Z. P. Li, Y. Z. Huang, S. P. Zhang, P. Nordlander, N. J. Halas, and H. X. Xu, *Nano Lett.* **10**, 1950–1954 (2010).
- [34] H. Wei, Z. X. Wang, X. R. Tian, M. Kall, and H. X. Xu, *Nat. Commun.* **2**, 387 (2011).
- [35] A. Drezet, A. Hohenau, D. Koller, A. Stepanov, H. Ditlbacher, B. Steinberger, F. R. Aussenegg, A. Leitner, and J. R. Krenn, *Mater. Sci. Eng. B-Adv. Funct. Solid-State Mater.* **149**, 220–229 (2008).
- [36] M. X. Song, A. Bouhelier, P. Bramant, J. Sharma, E. Dujardin, D. G. Zhang, and G. Colas-des-Francis, *ACS Nano* **5**, 5874–5880 (2011).
- [37] S. P. Zhang, and H. X. Xu, *ACS Nano* **6**, 8128–8135 (2012).
- [38] T. Shegai, V. D. Miljkovic, K. Bao, H. X. Xu, P. Nordlander, P. Johansson, and M. Kall, *Nano Lett.* **11**, 706–711 (2011).
- [39] H. A. Atwater and A. Polman, *Nat. Mater.* **9**, 205–213 (2010).
- [40] Y. Liu, R. Cheng, L. Liao, H. L. Zhou, J. W. Bai, G. Liu, L. X. Liu, Y. Huang, and X. F. Duan, *Nat. Commun.* **2**, 579 (2011).
- [41] H. Wei, S. P. Zhang, X. R. Tian, and H. X. Xu, *Proc. Natl. Acad. Sci. USA* **110**, 4494–4499 (2013).
- [42] M. A. Lieb, J. M. Zavislan, and L. Novotny, *J. Opt. Soc. Am. B* **21**, 1210–1215 (2004).